Role of active stress and linear turnover in biological systems

Shubham Anand
MS15208

A dissertation submitted for the partial fulfilment
of BS-MS dual degree in Science

Indian Institute of Science Education and Research Mohali
May 2020

Certificate of Examination

This is to certify that the dissertation titled **"Role of active stress and linear turnover in biological systems"** submitted by **Shubham Anand** (Reg. No. MS15208) for the partial fulfillment of BS-MS dual degree programme of the Institute, has been examined by the thesis committee duly appointed by the Institute. The committee finds the work done by the candidate satisfactory and recommends that the report be accepted.

Dr. Sanjeev Kumar Dr. Rajeev Kapri Dr. Abhishek Chaudhuri
(Supervisor)

Dated: June 15, 2020

Declaration

The work presented in this dissertation has been carried out by me under the guidance of Dr. Abhishek Chaudhuri at the Indian Institute of Science Education and Research Mohali.

This work has not been submitted in part or in full for a degree, a diploma, or a fellowship to any other university or institute. Whenever contributions of others are involved, every effort is made to indicate this clearly, with due acknowledgement of collaborative research and discussions. This thesis is a bonafide record of original work done by me and all sources listed within have been detailed in the bibliography.

Shubham Anand
(Candidate)

Dated: June 15, 2020

In my capacity as the supervisor of the candidate's project work, I certify that the above statements by the candidate are true to the best of my knowledge.

Dr. Abhishek Chaudhuri
(Supervisor)

Acknowledgment

Foremost, I would like to express my sincere gratitude to my thesis supervisor Dr. Abhishek Chaudhuri for the continuous support of MS thesis, for his patience, motivation, enthusiasm and immense knowledge. He has taught me the methodology to carry out the research and to present the research works as clearly as possible. It was a great privilege and honour to work and study under his guidance. I am incredibly grateful for what he has offered me. His weekly discussions were constructive to correct me where I'm doing wrong in research. I would also like to thank him for his friendship, empathy, and a great sense of humour.

Besides my advisor, I would like to thank the rest of my thesis committee: Dr. Sanjeev Kumar and Dr. Rajeev Kaprifor their encouragement, insight comments during a poster presentation. I want to extend my sincere gratitude to Dr.Vijaykumar Krishnamurthy from the International Centre for Theoretical Science, Bengaluru(ICTS), for taking the time to correct my mistakes, guiding me in my research and offering summer internship opportunity to work with there group and leading me working on diverse, exciting projects.

I would also thank my fellow lab mates for the helpful discussions, support during my research and the fun we had during my stay at Indian Institute of Science, Education and Research, MOHALI and some lab members from ICTS, Bengaluru for there constant support.

I have made friends here, which are more like my family for the rest of my life. The fun we had during our stay in college are the moments to cherish. I want to thank all my friends, who always helped me and guided me to be a better person in my life. Deepanshu and Shubham Gajrani my two pillars which were still there to help me during my odd time and offering there criticism when needed. I want to thank Nikhil Tanwar for always helping me in studies and having a good time. Saurabh Bedi for always coming a day before exams and making me revise all the stuff and helping in all the Bad situations and thanking my dearest friends Deepti, Disha, Yogesh, Sourabh soni, Amit, Aman, Ritwik and my Bhangra buddies for a cherishable time.

I dedicate this work to my parents. I will always be indebted to them, and I cannot thank them enough for their constant support, faith and encouragement. I am extremely grateful to my parents for their love, prayers, caring and sacrifices for educating and preparing me for my future. Finally, I would like to thank IISER MOHALI for all the facilities and DST-INSPIRE for the financial support.

List of Figures

Abstract

We show the pattern formation in living systems by incorporating the simplest models. Mechanochemical patterning was the main aim of consideration to describe the morphogenesis process. Firstly, we showed the pattern formation for single chemical species in one - dimension with the help of active stress and linear turnover. The chemical species was active stress up regulator. Active stress leads to the non-homogeneous concentration profile with the help of hydrodynamic flows generated and having spontaneous stationary patterns. Then we had a linear turnover in the advection-diffusion system for the single diffusing chemical species which showed travelling and oscillatory patterns as well as stabilization of multiple peaks in the concentration profiles. We then showed pattern formation for two chemical species in one-dimension. Here, one was active stress up-regulator diffusing fastly, and other was active stress down-regulator diffusing slow. This system showed pulsatory patterns. Afterwards, we incorporated linear turn over into the advection-diffusion system where we observe patterns only if active stress up regulator turns over fast as compared to active stress down regulator, for which turnover is slow. The whole work is motivated by the two PRL papers cited in the reference.

Contents

Chapter 1

Introduction

Pattern formation is a fundamental property of life and is a beautiful phenomenon. Patterns are seen everywhere in the physical world and in living systems ; also, they vary from being simple to complex. We have seen patterns like in peacock feathers, leopard spots, zebra stripes, water waves, rock layers and dunes. Patterns can be seen in non-living systems also. The most exciting part of pattern formation is observed for biological systems during the generation of complex organisms which is called morphogenesis. Morphogenesis process got the attention of many scientists about the question that how pattern formation in this process can be understood from physics principles.

1.1 Some fundamental aspects of Pattern formation

The human eye is always bored with monotonous views. Complexity always attracts us, which occurs spontaneously, especially spatiotemporal complexity [2]. We will be looking at such systems which are changing with spatial coordinates as well as time. For example, many patterns established have different time and length scales associated with them due to various conditions. It is seen when the embryo is getting developed; there are multiple shapes observed on it. Alan Turing discussed in his paper that this process can be best explained by a reaction-diffusion system where two chemical species are reacting with each other and diffusing with the difference in their diffusion rates which leads to different concentration profiles [3].

The chemical species which govern the morphogenesis process are called morphogens. These morphogens where one is an activator and other inhibitor are adequate for morphogenesis process when the system is disturbed from its unstable homogeneous state by various chemical signals. Alan Turing, in his paper, only discussed the pattern formation due to the chemical part. He neglected the mechanical part, which is also an essential part for morphogenesis.

1.2 The mathematical equation for reaction-diffusion systems

For seeing different kinds of pattern formation for the chemical part, we need various chemical species which are reacting and diffusing in the system from their initial uniform state - this results in different concentration profiles which depends upon the space and time.

Let us first consider a chemical species whose concentration is varying spatiotemporally $c(x,t)$, in a one dimensional system. Diffusion here plays an important part where concentration is dependent on the diffusion constant represented by D. These kinds of system are best represented by Fick's equation where net flux J_x at x and t is directly proportional to the concentration gradient. where proportionality constant is D [4].

$$J_x = -D\frac{\partial c}{\partial x} \tag{1.1}$$

This is Fick's first equation. For the concentration of chemical species, we can write the continuity equation, which is the second equation.

$$\frac{\partial c}{\partial t} = -\frac{\partial J_x}{\partial x} \tag{1.2}$$

Here the concentration is going from a high concentration region to low concentration region. But for the reaction-diffusion system, reaction is also playing a vital role. Reaction rate $r(c, c_1, c_2, c_{3,.....})$ is also affecting the rate of change of concentration for chemical species where r is the reaction rate due to interaction with other chemical

species with concentrations $c_1, c_2, ...$ Therefore, Eq. 1.2 gets modified to

$$\frac{\partial c}{\partial t} = -\frac{\partial J_x}{\partial x} + r(c, c_1, c_2.c_{3,.....}) \tag{1.3}$$

When we combine equations Eq. 1.3 and Eq. 1.2 we get the equation for rate of change of concentration in reaction diffusion systems :

$$\frac{\partial c}{\partial t} = D\frac{\partial^2 c}{\partial x^2} + r(c, c_1, c_2, c_{3,.....}). \tag{1.4}$$

Alan Turing suggested that at least two chemical species are required to observe patterns [3] and their diffusion constants should have meaningful difference. For higher dimension the same equation is written in the form :

$$\frac{\partial c}{\partial t} = D\nabla^2 c + r(c, c_1, c_2, c_{3,.....}). \tag{1.5}$$

For three dimension ∇^2 can be written as $\nabla^2 \rightarrow \partial_x^2 + \partial_y^2 + \partial_z^2$.

1.3 Linear stability analysis for Turing systems

As we discussed earlier, we require at least two chemical species for forming patterns in Turing system, but is it a sufficient condition? Equations described for reaction-diffusion systems are evolving in time and space. These systems form pattern when they are perturbed from their homogeneous state only if it is an unstable state. To see whether the initial uniform state is stable or not, we do linear stability analysis [5].

Let us consider two chemical species in a reaction-diffusion system which is represented by the given set of equations below.

$$\frac{\partial u}{\partial t} = D_u\frac{\partial^2 u}{\partial x^2} + R_1(u, v) \tag{1.6}$$

$$\frac{\partial v}{\partial t} = D_v\frac{\partial^2 v}{\partial x^2} + R_2(u, v) \tag{1.7}$$

where R_1, R_2 are the reaction rates for the interacting chemical species and D_u, D_v are the respective diffusion constants. For calculating homogeneous state put equation (1.6) and (1.7) equal to 0 which leads to $R_1(u, v) = 0$ and $R_2(u, v) = 0$. Solving them gives the homogeneous state given by (u^*, v^*) simultaneously. For performing

linear stability analysis, we perturb our homogeneous state by the small perturbation $u \to u^* + u_p, v \to v^* + v_p$. Then,

$$\partial_t(u^* + u_p) = D_u \partial_x^2(u^* + u_p) + R_1(u^* + u_p, v^* + v_p) \tag{1.8}$$

$$\partial_t(v^* + v_p) = D_v \partial_x^2(v^* + v_p) + R_2(u^* + u_p, v^* + v_p). \tag{1.9}$$

For the reaction part, we do Taylor series expansion about the homogeneous state up to the linear terms and neglect higher-order terms for simplicity.

$$\partial_t(u_p) = D_u \partial_x^2(u_p) + R_{1u} u_p + R_{1v} v_p \tag{1.10}$$

$$\partial_t(v_p) = D_v \partial_x^2(v_p) + R_{2u} u_p + R_{2v} v_p \tag{1.11}$$

where, $R_{ij} = \frac{\partial R_i}{\partial j}$ and $i = 1, 2, j = u, v$. Further, the equation is linear with constant coefficients and also the boundary conditions are periodic or at infinity. For finding the exact form of the perturbed state we use Fourier analysis which leads to the following solution [5].

$$X_p = X_k e^{\lambda_k t} e^{\iota k x} = \begin{pmatrix} u_k \\ v_k \end{pmatrix} e^{\lambda_k t} e^{\iota k x} \tag{1.12}$$

Here $X_p = \begin{pmatrix} u_p \\ v_p \end{pmatrix}$ is the perturbed state, X_k is the constant vector and k is Fourier mode. Let us substitute this expression of perturbed state in equations Eqs. 1.10 and 1.11 and collect the terms to get an eigenvalue problem :

$$A_k X_k = \lambda_k X_k \tag{1.13}$$

Here, $\boldsymbol{A}$ is the real 2×2 matrix.

$$\boldsymbol{A} = \begin{pmatrix} R_{1u} - k^2 D_u & R_{1v} \\ R_{2u} & R_{2v} - k^2 D_v \end{pmatrix} \tag{1.14}$$

After solving the eigenvalue equation, we get two linearly independent eigenvectors $\boldsymbol{u_p}$ and $\boldsymbol{v_p}$ with corresponding eigenvalues λ_{1k} and λ_{2k}.

$$X_k = c_1 \boldsymbol{u_p} e^{\lambda_{1k}} + c_2 \boldsymbol{v_p} e^{\lambda_{2k}} \tag{1.15}$$

If both the eigenvalues calculated are such that $\mathrm{Re}\lambda_{ik} < 0$ for i = 1, 2 then the perturbation will decay and the system comes back to its original homogeneous state. But as we know, the perturbation solution is the combination over all the Fourier modes, so if this condition is true $\boldsymbol{max_i max_k \lambda_{ik}} < 0$ then the homogeneous state is stable.

For calculating the eigenvalues, we solve the following equation.

$$det(\boldsymbol{A_k} - \lambda_k \boldsymbol{I}) = 0 = \lambda_k^2 - (Tr\boldsymbol{A_k})\lambda_k + det\boldsymbol{A_k} \tag{1.16}$$

Solving this quadratic equation gives the value of the eigenvalues.

$$\lambda_k = \frac{1}{2} Tr\boldsymbol{A_k} \pm \frac{1}{2}\sqrt{(Tr\boldsymbol{A_k}^2) - 4det\boldsymbol{A_k}} \tag{1.17}$$

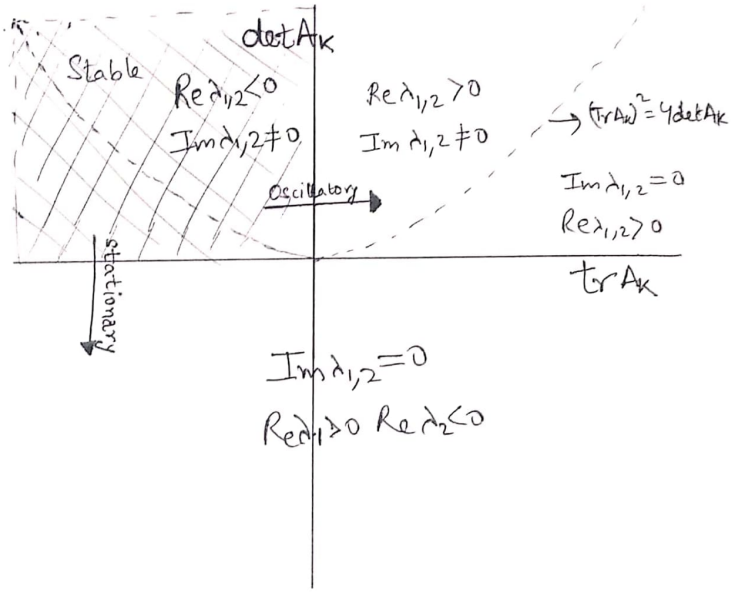

Figure 1.1: Different regions of Turing system in $Tr\boldsymbol{A_k} - det\boldsymbol{A_k}$ plane.

From the Fig. 1.1, we can see that if $Tr\boldsymbol{A_k} < 0$ and $det\boldsymbol{A_k} > 0$ then we have a stable region. These conditions lead to some constraint for all Fourier modes.

$$Tr\boldsymbol{A_k} = R_{1u} + R_{2v} - (D_u + D_v)k^2 < 0 \tag{1.18}$$

$$det\boldsymbol{A_k} = (R_{1u} - D_u^2)(R_{2v} - D_v k^2) - R_{1v}R_{2u} > 0 \tag{1.19}$$

1.3.1 Physical insights

Let us for the Turing system switch off the diffusion constant which implies stirring the solutions at a fast rate. We find that Eqs. 1.18, 1.19 leads to $R_{1u} + R_{2v} < 0$ and $R_{1u}R_{2v} - R_{1v}R_{2u} > 0$ for the stability of uniform state when perturbed. Further, If we include the diffusion constant, then the same equation 1.18 for the trace remains less than zero for different modes. But the Eq. 1.19 behaves differently when we include diffusion constants.

The $det\boldsymbol{A_k}$ is an upward parabola for k^2 when the sign of this change which we can see from the fig. 1.1 then there are stable patterns observed in the system at a minimum Fourier mode k_m when $det\boldsymbol{A_k}$ is minimum for k^2.

$$K_m = \frac{D_u R_{2v} + D_v R_{1u}}{2D_u D_v} \tag{1.20}$$

From $R_{1u} + R_{2v} < 0$ and (1.20), we obtain that one is an activator, and other is an inhibitor for the patterns to get formed. let $R_{1u} > 0$ be an activator, and $R_{2v} < 0$ be an inhibitor. Moreover, for the Turing instability diffusion constant of inhibitor should be higher from the diffusion constant of activator by at least one order ($\frac{D_v}{D_u} > 1$) [6] which is also refered as "Local activation with long-range inhibition".

Chapter 2

Role of active stress and turnover in pattern formation for one chemical species

Embryo development is a fascinating process if we see from the physics point of view. This developmental process is a tight integration of mechanical forces and biochemical signalling [1]. In 1952, Alan Turing suggested that reaction-diffusion equations can best describe this pattern formation in multicellular organisms. Still, he also mentioned about the mechanical effect, which should also be taken into account. It has been seen in the development context that mechanical forces play a vital role in pattern formation and shaping the embryo (see Fig. 2.1). This mechanism generally happens at the cellular cytoskeleton cortex beneath the cell membrane. There is a connection between pattern formation and morphogenesis which can be explained by active mechanochemical patterning [1].

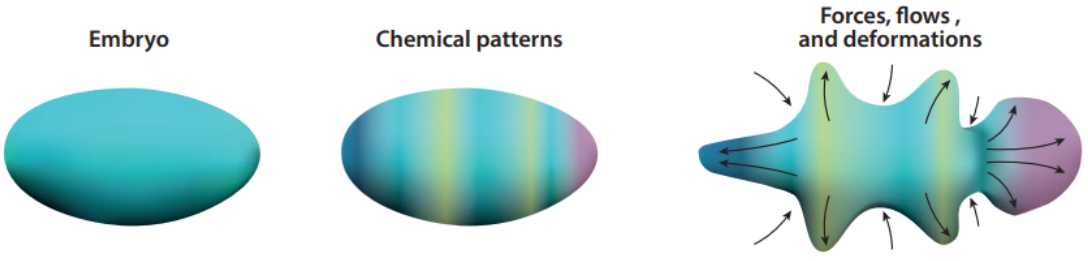

Figure 2.1: Embryo development first encounters pattern formation followed by the shape change due to mechanical stresses regulated by biochemical signalling proteins hence increasing spatial complexity.Taken from [1]

Talking about the cytoskeleton, it consists of a meshwork of filamentous proteins called cytoskeleton filaments such as actins and microtubules and molecular motors like myosin. Myosin motors are considered as active matter as they have self-propelled movement on actin filaments by consuming energy from the ATP(adenosine triphosphate) hydrolysis. Myosin motors lead to a contraction in the actin filaments by cross-linking them. More the myosin motors in a particular area larger is the contraction leading to mechanical stress on long length scales, reaching up to the cellular and tissue scale (see Fig. 2.2). This mechanical forces which are being generated in the cellular cytoskeleton take the system far from thermal equilibrium.

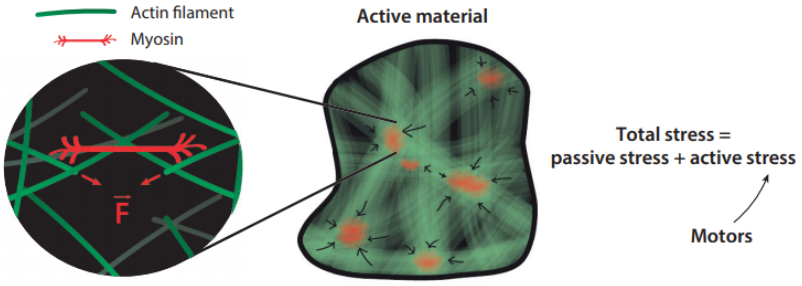

Figure 2.2: The figure shows the mechanics happening at the cellular scale in the actomyosin cortex(which is beneath the cell membrane), leading to additional active stress.Taken from [1]

2.1 Mechanical aspect of pattern formation

Cells and tissues show a beautiful property of autonomously generating forces. Active mechanical stresses play a crucial role in pattern formation for developing multicellular organism. So, here we present a model which involves the mechanical part. This model was given by Bois et. al. [7].

Here, actomyosin cortex (a thin cytoskeleton meshwork) is considered as an active fluid for specific time scales. The reason for choosing it as an active viscous fluid is because for time scale for turnover happening with the cytoplasm is very much less than the time scale for which it is behaving like a fluid. The main aim of this paper was to look for the pattern formation in an active fluid with only one chemical species with hydrodynamical flows generated. In Turing system, we needed at least two reaction-diffusion equations for pattern formation. Here we need only one advection-diffusion equation as actively generated hydrodynamic flows leads to the advection

of chemical species which upregulates the active stress. These flows are generated if there is spatial inhomogeneity of active stress profiles.

Let us consider a thin film of active fluid which is having a constant thickness as we have in actomyosin cortex which is maintained by exchanging the material with the cytoplasm. Movement is taken only in one-dimension along the x-axis. In this model, we consider only one chemical species. The concentration of the regulator $c(x,t)$ (like myosin in the cytoskeleton) is given by the conservation equation (equation of continuity) in one dimension. It involves a diffusion component (diffusion constant D) and an advective component. Advective part comes due to the flow of regulatory species with a velocity v.

$$\partial_t c = -\partial_x j \tag{2.1}$$

$$j = -D\partial_x c + vc \tag{2.2}$$

where j is the flux for the regulatory species. Mechanical effect is included in the form of mechanical stress. For the hydrodynamic flows, the total stress part in actomyosin cortex is given by

$$\sigma = \sigma_p + \sigma_a \tag{2.3}$$

$$= \eta\partial_x v + (\zeta\Delta\mu)_0 f(c) \tag{2.4}$$

where σ_p is the passive stress, caused by the viscosity of the fluid (η : viscosity) and σ_a is the active stress which arises due to the molecular motor activity and is dependent on the concentration of the chemical species. It is an isotropic stress meaning it has the same value in different directions. Active stress is positive for contraction and is dependent on the change in the chemical potential ($\Delta\mu$) by ATP hydrolysis. $f(c)$ is the function which depends upon the concentration.

At the cellular scale, Reynold's number is low, so for the actomyosin cortex, we can neglect the inertial forces (viscocity is very high) which leads to a force balance equation on the fluid element. Force balance equation is written as follows :

$$\nabla \cdot \sigma = \gamma \boldsymbol{v} \tag{2.5}$$

where γ is the friction coefficient of the thin layer, which describes the friction between

the layer and the cell membrane or substrate. As the system is in one-dimension, so the force balance equation changes to,

$$\partial_x \sigma = \gamma v. \tag{2.6}$$

Active stress and force balance equation can be simplified further by substituting (2.4) in (2.6), which leads to an equation where velocity is dependent on the concentration of the regulator.

$$\eta \partial_x^2 v - \gamma v = -(\zeta \Delta\mu)_0 \partial_x f(c) \tag{2.7}$$

The function $f(c)$ which is dependent on the concentration is taken to be of the form $c/(c+1)$. It is also known as Hill's equation this function shows saturation after some time and $\partial_c f(c_0) > 0$ which means active stress is up regulated by the regulator. Eqn 2.1 can be simplified further which gives advection-diffusion equation

$$\partial_t c = -\partial_x (vc) + D\partial_x^2 c \tag{2.8}$$

Eqs. 2.7 and 2.8 are two coupled equations where concentration and velocity are dependent on each other. Solving the equations above simultaneously gives the desired mechanochemical pattern in 1-D.

2.2 Linear stability analysis for the steady state

To obtain the criterion for stationary stable patterns from a homogeneous steady state, we perform a linear stability analysis about the steady-state which is $c = c_0$ and $v = 0$. Here stable states are perturbed with small perturbation. The perturbations are

$$c = c_0 + c_p \qquad v = v_p \tag{2.9}$$

$c_p = \delta c = \delta c_0 e^{q_k t + \iota k x}$ and $v_p = \delta v = \delta v_0 e^{q_k t + \iota k x}$ where $K = \pm \frac{\beta n \pi}{L}$ is the wave number for the spatial perturbation with $n \in \mathbb{Z}$. Consider equation (2.4) with perturbed state.

Taylor expanding the function $f(c_0 + \delta c)$ till linear order terms we get [7],

$$\sigma = \eta \partial_x v + (\zeta \Delta\mu)_0 f(c_0 + \delta c) \tag{2.10}$$

$$= \eta \partial_x v + (\zeta \Delta\mu)_0 (f(c_0) + \partial_c f(c_0)\delta c). \tag{2.11}$$

. Substitute this in the equation (2.6) and performing the Fourier transform, we get

$$(\eta k^2 + \gamma) v = (\zeta \Delta\mu)_0 \partial_c f(c_0) \iota k \delta c. \tag{2.12}$$

From Eq. 3.8 we obtain velocity as,

$$v(k) = \frac{(\zeta \Delta\mu)_0 \partial_c f(c_0) \iota k \delta c}{(\eta k^2 + \gamma)}. \tag{2.13}$$

Insert Eq. 2.13 into Eq. 2.8 and taking only linear order terms, we get the eigenvalue $\lambda(k)$ of the form which is the dispersion relation. Some parameters which are necessary for the dispersion relation are defined as $Pe = \frac{(\zeta\Delta\mu)_0}{D\gamma} = \frac{Ul}{D}$, where $U = \frac{(\zeta\Delta\mu)_0}{\sqrt{\eta\gamma}}$. Pe is the Peclet number which is the ratio of diffusive to advective time scales, $l = \sqrt{\frac{\eta}{\gamma}}$ is the characterisitic length [8]. The eigenvalue is obtained as

$$\lambda(k) = -k^2 D (1 - \frac{Pe c_0 \partial_c f(c_0)}{1 + k^2 l^2}). \tag{2.14}$$

This dispersion relation is the main governing factor for spontaneous pattern formation from the uniform steady state. If the steady-state is unstable then when we perturb the state, it forms a pattern, and the condition for the eigenvalue is it should be positive for some k. The condition which needs to be fulfilled for eigenvalue to be positive for periodic boundary condition and when the wave number $k = \frac{2\pi}{L}$ (L : domain size) is as follows

$$\frac{Pe c_0 \partial_c f(c_0)}{1 + (\frac{2\pi l}{L})^2} > 1. \tag{2.15}$$

If we take $\frac{L}{l} = x\pi (x \in \mathbb{Z})$ then the condition for the minimum Pe from which we start observing patters for some k is

$$Pe = (1 + \frac{4}{x^2}) \frac{(1 + c_0)^2}{c_0}. \tag{2.16}$$

2.3 Numerical solution and Analysis

We took the two coupled equations Eqs. 2.7 and 2.8 and solved them numerically in python with the help of Fourier transform method, which is mentioned in the Appendix-A. Following were the plots observed for the periodic boundary condition where $x \in [0, L]$.

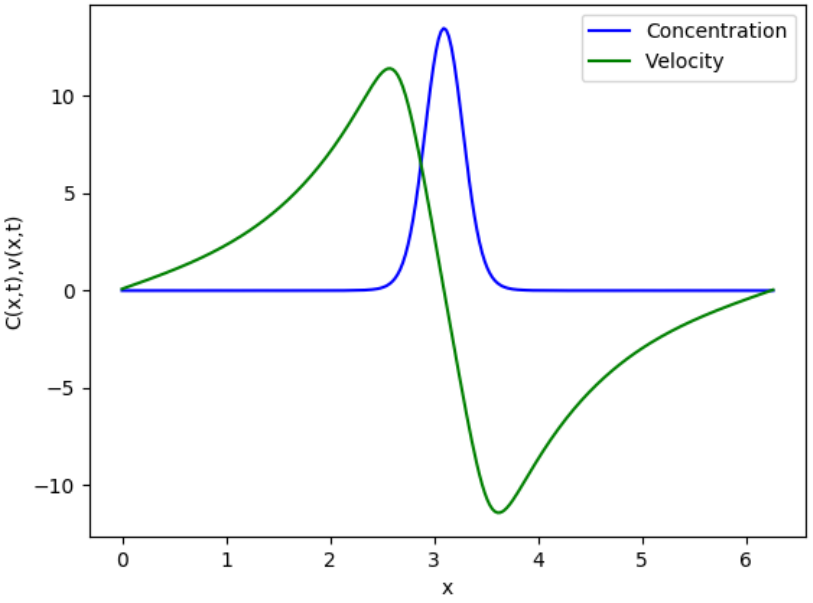

Figure 2.3: Concentration and velocity profile at steady state for $\frac{L}{l} = 2\pi$, $c_0 = 1$ and $Pe = 16$.

Fig. 2.3 shows the emergence of stationary patterns. Concentration profile evolution is seen due to the advection and diffusion part. We can see that the velocity profile is crossing the zero at the extremum of the concentration profile showing that the flow of regulator is into the peaks and out of the valleys [7]. Diffusion tries to smooth the concentration profile while advection leads to clumping due to non- homogeneous active stress profile. Stationary patterns are observed when the advective flux balances the diffusive flux at some point.

$$\lambda(k) = -k^2 D(1 - \frac{Pec_0\partial_c f(c_0)}{1 + k^2 l^2}) \tag{2.17}$$

In Fig. 2.4, we look at the dispersion relation (Eq. 2.14) for different activity by

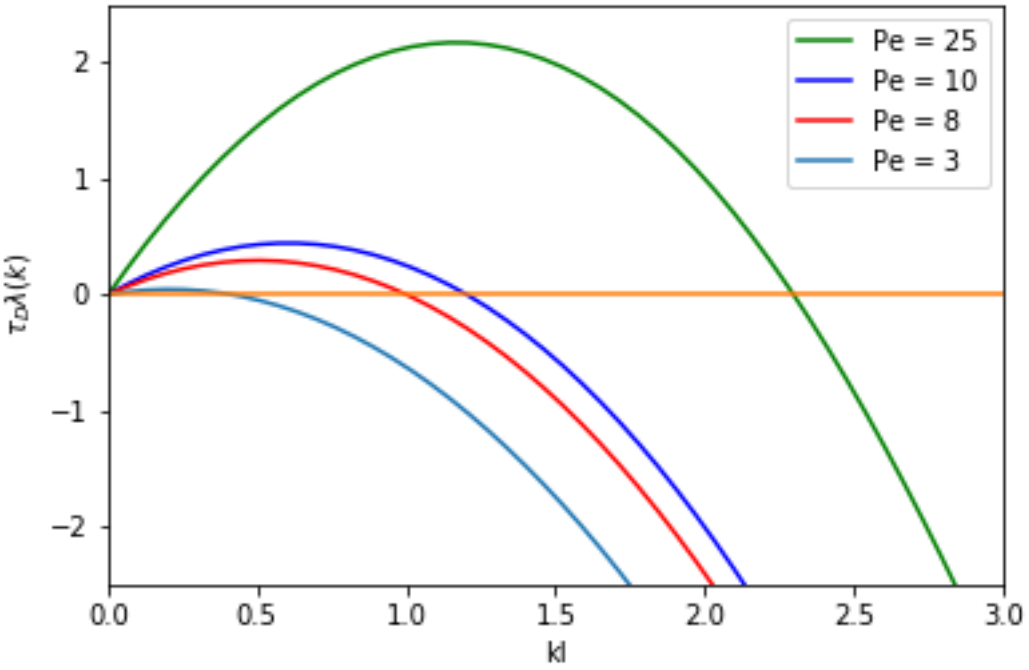

Figure 2.4: Dispersion relation ($\lambda(k)$) for $Pe = 3, 8, 10$ and 25 after performing linear stability analysis. The eigenvalue $\lambda(k)$ is non-dimensionalized by the diffusive time scales $\tau_D = \frac{l^2}{D}$

varying Pe. We have already established that there is a critical value of Pe after which the eigenvalue is positive and patterns starts to form. Patterns grow when $\lambda(k)$ is maximal for wavenumber k. For low Pe, $\lambda(k)$ is negative for all k. With increasing Pe, the regime of postive $\lambda(k)$ emerges.

For a given set of parameters system, we can sometimes get multiple peaks at the start. However, these are not steady states. If we wait for long time, then these multiple peaks disappear and we get single peak. In Fig. 2.5, we see the situation for $\frac{L}{l} = 5\pi$ where there are three peaks initially. As time progresses, the peaks merge and form a single stable peak.

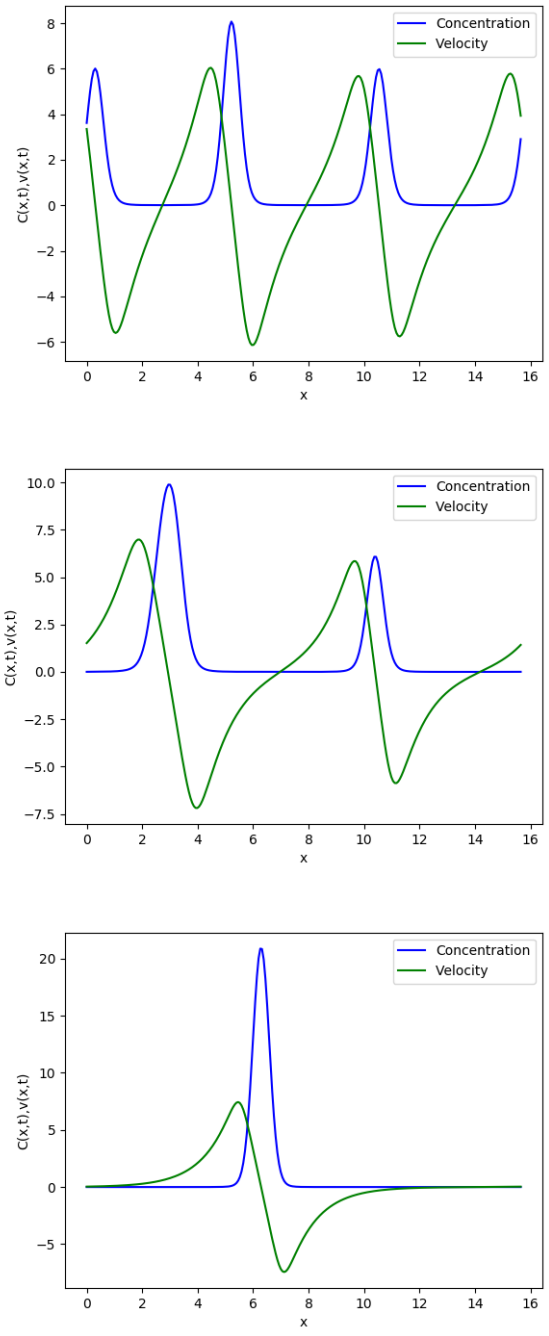

Figure 2.5: Concentration and velocity profile at steady state for $\frac{L}{l} = 5\pi$, $c_0 = 1$ and $Pe = 16$, system goes from multipeak to single peak (top to bottom).

2.4 Pattern formation in active fluid with linear turnover

Here we consider pattern formation in a thin film of active fluid with linear turnover rate R. The tunrnover can be motivated as actin filaments polymerizing and depolymerizing. The equations get slightly changed as chemical kinetics is also having a contribution to the concentration change of the chemical species.

$$\partial_t c = D\partial_x^2 c - \partial_x(vc) - R(c - c_0), \tag{2.18}$$

$$\eta\partial_x^2 v - \gamma v = -(\zeta\Delta\mu)_0\partial_x f(c) \tag{2.19}$$

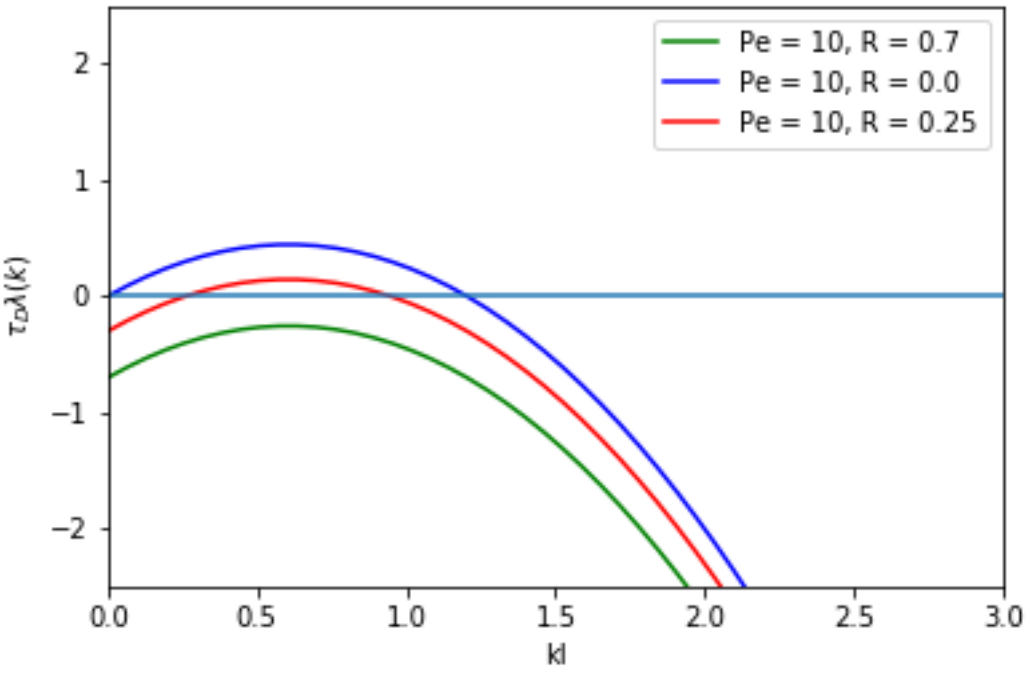

Figure 2.6: Dispersion relation $\lambda(k)$ for $Pe = 10$ for $R = 0, 0.25$ and 0.7. The eigenvalue $\lambda(k)$ is made dimensionless by the diffusive time scales $\tau_D = \frac{l^2}{D}$.

0.5cm

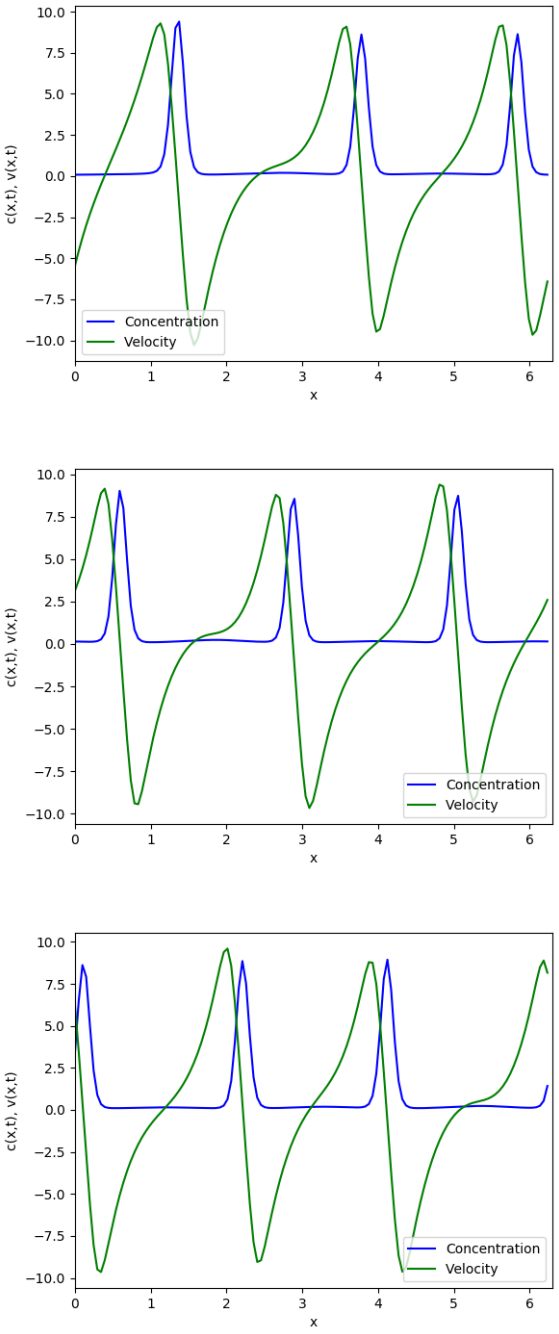

Figure 2.7: Travelling of pattern from right to left seen for different times at $\frac{L}{l} = 5\pi$, $c_0 = 1$, $Pe = 50, R = 0.5$.

We can again do the linear stability analysis in the presence of turnover and get the dispersion relation. In this case we obtain the $\lambda(k)$ as

$$\lambda(k) = -k^2 D \left(1 - \frac{Pec_0 \partial_c f(c_0)}{1 + k^2 l^2}\right) - R. \tag{2.20}$$

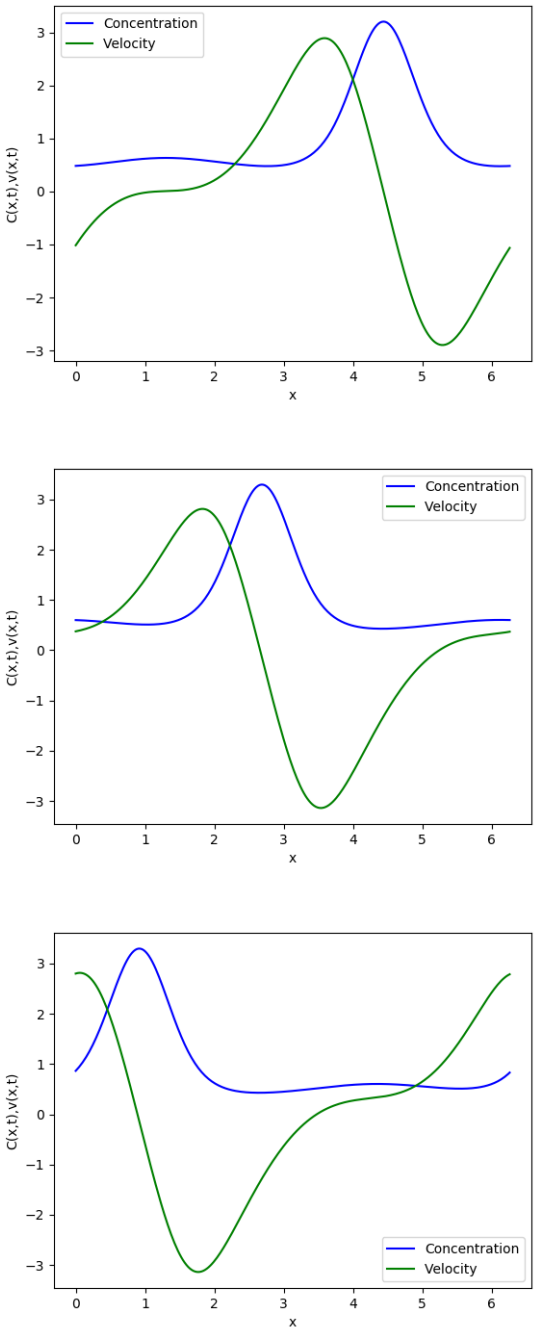

Figure 2.8: Travelling of pattern from right to left seen for different times at $\frac{l}{L} = 2\pi$, $c_0 = 1$ and $Pe = 25$.

In Fig. 2.6, we plot $\lambda(k)$ as function of k for different Pe and R values. As we can see, at a given Pe, the dispersion curve is shifted downward when the linear turnover rate is increased. Therefore, the critical Pe required for patterning to be observed is

more as compared to the case $R = 0$. Indeed the condition for critical Pe is obtained from

$$\frac{Pe_c c_0 \partial_c f(c_0)}{1 + (\frac{2\pi l}{L})^2} = 1 + \frac{R}{(\frac{2\pi}{L})^2 D}. \tag{2.21}$$

We observe two interesting things when $R \neq 0$. Firstly, for the parameters where multiple peaks were observed to merge in the $R = 0$ case, multiple peaks are now found to be stable and they do not merge. This can be seen in Fig. 2.7. Here the three peaks that are observed initially do not merge into a single peak even at long times. Therefore, multiple peaks are stabilized.

The other interesting feature is that for certain parameters, the peaks that are formed are not stationary but are moving and oscillating. The peaks do not merge to form single peak, but there are oscillations in the system with peaks going down and appearing in regions where there were no peaks. In Fig. 2.8, we plot the concentration and velocity distributions at different times to show this behavior.

Chapter 3

Role of active stress for two chemical species

In the previous chapter we have seen that patterns can form even in the absence of chemical instabilties as proposed by Turing. The patterning is brought about by activity. In this chapter we will explore what happens when on top of activity we have two types of chemical species with one being the activator and the other an inhibitor. In this case we see pulsatory patterns [9].

3.1 Two chemical species and activity

Consider two chemical species one is activator with concentration profile $A(x,t)$ and other is inhibitor with concentration profile $I(x,t)$ dependent on position x and time t. They both are taken in an active film of finite length L in one-dimension. Concentration evolution is considered with the help of advection and diffusion terms.

$$\partial_t A = -\partial_x(vA) + D_1\partial_x^2 A, \tag{3.1}$$

$$\partial_t I = -\partial_x(vI) + D_2\partial_x^2 I, \tag{3.2}$$

where D_1 and D_2 are the diffusion constants for the two chemical species and v is the hydrodynamic flow velocity. We let $D_2/D_1 = \alpha > 0$.

The stress is again divided into the passive and active parts with the active stress being independent of the chemical species. Therefore, for both activator and inhibitor, $\sigma_a = (\zeta\Delta\mu)_0 f(c)$. However, $f(c)$ is now a function of both activator and inhibitor

concentrations and obeys the Hill form

$$f(c) = (1+\beta)\frac{A}{A+A_m} + (1-\beta)\frac{I}{I+I_m}. \tag{3.3}$$

Here A_m and I_m are the values when saturation is reached and β is an asymmetry parameter.

3.2 Linear stability analyses for the steady state

. Let us consider the homogeneous steady state for the system under consideration where concentration is $c_0 = (A_0, I_0)$ and velocity is $v = 0$. To see whether the steady state is stable or unstable we perturb it from the steady state. Perturbations are taken of the form $c = c_0 + \delta c_0 e^{\iota kx}$. Consider equation (2.4) with perturbed state and Taylor expanding the function $f(c_0 + \delta c)$ upto linear terms.

$$\begin{aligned}
\sigma &= \eta\partial_x v + (\zeta\Delta\mu)_0 f(c_0 + \delta c) && (3.4)\\
&= \eta\partial_x v + (\zeta\Delta\mu)_0 f(A_0 + \delta A, I_0 + \delta I) && (3.5)\\
&= \eta\partial_x v + (\zeta\Delta\mu)_0 (f(A_0, I_0) + \partial_A f\delta A + \partial_I f\delta I) && (3.6)
\end{aligned}$$

.
Substitute this in the equation (2.6) and perturbed state of v we get.

$$\begin{aligned}
\eta\partial_x^2 v + (\zeta\Delta\mu)_0(\partial_A f\delta A + \partial_I f\delta I)\iota k &= \gamma v && (3.7)\\
(\eta k^2 + \gamma)v &= (\zeta\Delta\mu)_0(\partial_A f\delta A + \partial_I f\delta I)\iota k && (3.8)
\end{aligned}$$

From (3.8) we obtain velocity as.

$$v(k) = \frac{(\zeta\Delta\mu)_0(\partial_A f\delta A + \partial_I f\delta I)\iota k}{\gamma(1 + k^2 l^2)} \tag{3.9}$$

Now, take equations (3.1) and (4.2) with perturbed state and considering only linear

order terms we get,

$$\partial_t(\delta A) = -\iota k v(k) A_0 - k^2 D \delta A, \tag{3.10}$$

$$\partial_t(\delta I) = -\iota k v(k) I_0 - k^2 D \delta I. \tag{3.11}$$

Now, as we substitute value of $v(k)$ into equations (3.10) and (3.11), we get an eigen value equation with a 2×2 stability matrix given as

$$\tau \mathbb{L} = -k^2 l^2 \begin{pmatrix} 1 & 0 \\ 0 & \alpha \end{pmatrix} + \frac{Pe k^2 l^2}{1 + k^2 l^2} \begin{pmatrix} A_0 f_A & A_0 f_I \\ I_0 f_A & I_0 f_I \end{pmatrix}. \tag{3.12}$$

Here, $Pe = \frac{(\zeta \Delta \mu)_0}{\gamma D}$ and $\tau = \frac{l^2}{D}$ is a diffusive time scale. Also, $f_A \equiv \partial_A f(c_0), f_I \equiv \partial_I f(c_0)$. For finding the eigen values we set $det(\mathbb{L} - \lambda(k)\mathbb{I}) = 0$. As it is a 2 X 2 matrix there will two eigen values given by

$$\lambda_k = \frac{1}{2} Tr\mathbb{L} \pm \frac{1}{2} \sqrt{(Tr\mathbb{L}^2) - 4 det\mathbb{L}}. \tag{3.13}$$

The stability of the system will be determined from $tr\mathbb{L}$ and the discriminant $\Delta\mathbb{L} = (tr\mathbb{L})^2 - 4 det\mathbb{L}(det\mathbb{L}$:

$$tr\mathbb{L} = -Dk^2[(1+\alpha) - \Pi(k)(A_0 f_A + I_0 f_I)], \tag{3.14}$$

$$\Delta\mathbb{L} = D^2 k^4[(1-\alpha)^2 + \Pi^2(k)(A_0 f_A + I_0 f_I)^2 - 2\Pi(k)(1-\alpha)(A_0 f_A - I_0 f_I)] \tag{3.15}$$

with $\Pi = \frac{Pe}{(1+k^2 l^2)}$. For the homogeneous state to be unstable, largest eigen value of the linear stability matrix should have real part to be positive $Re[\lambda(k)] > 0$. The wave number is $k_n = \frac{2n\pi}{L}$ where L is the size of the system. The first mode k_1 becomes unstable when the Peclet number is increased above the critical value of Pe_c. In the previous chapter we saw that the instability was stationary. Here for having oscillatory instability we should have $tr\mathbb{L}(k_1) > 0$ and $\Delta\mathbb{L}(k_1) < 0$ (see Fig. 1.1). The critical Pe_c is obtained as

$$Pe_c = \frac{(1+\alpha)(1 + \frac{4\pi^2 l^2}{L^2})}{(A_0 f_A + I_0 f_I)} \tag{3.16}$$

We analyze the situations for the patterns to happen :

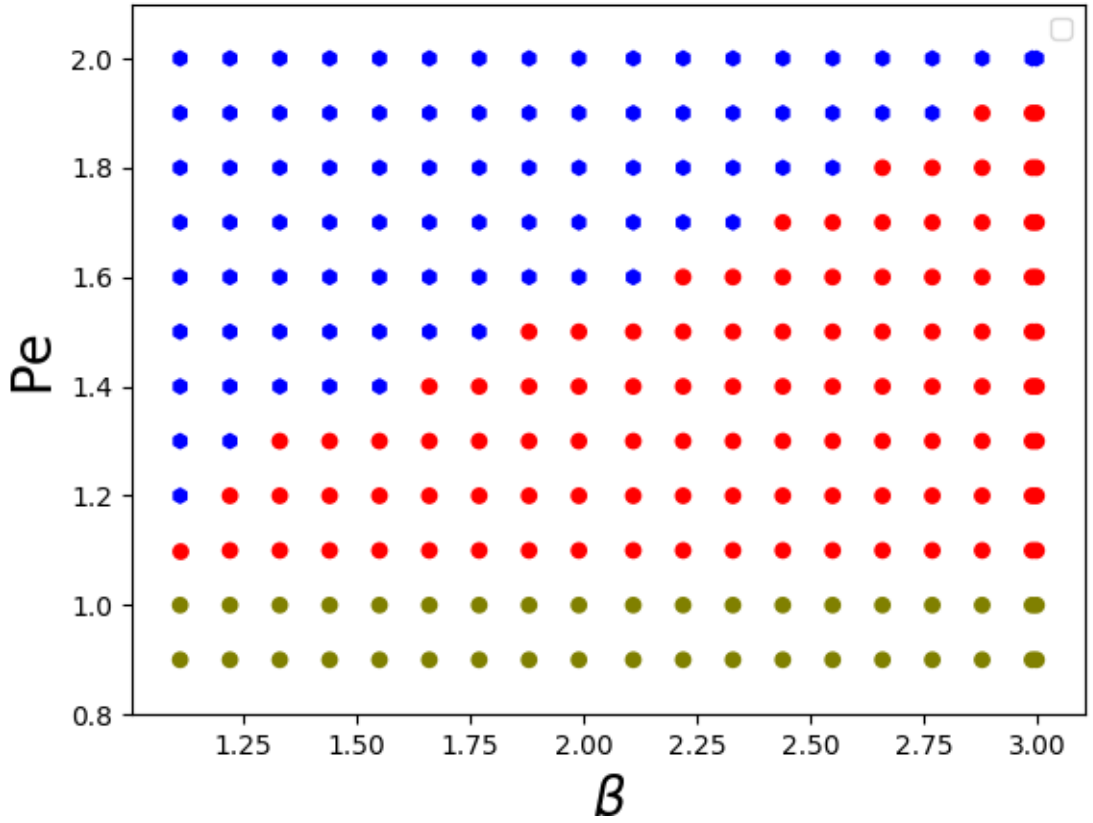

Figure 3.1: Phase Diagram for two-chemical species with $\alpha = 0.1$, and parameters which control the patterns are Peclet number (Pe) and β. Here blue colour points represent stationary patterns, Red colour points represent pulsatory patterns, and olive colour shows the homogeneous state.

- if $f_A > 0$ and $f_I < 0$ for $\alpha < 1$,or
- if $f_I > 0$ and $f_A < 0$ for $\alpha > 1$

For oscillatory instability, $f_A > 0$ implies that A is the stress up - regulator, while $f_I < 0$ implies that I is a stress down regulator. So, A diffuses faster as compared to I and $\alpha < 1$ [9]. These conditions are similar to what Turing defined for reaction-diffusion systems. Also, $\beta > 1$ when the above condition is applied to the regulator function of active stress. If both A and I have the same diffusion constants or both up-regulate the active stress, then there are stationary patterns formed.

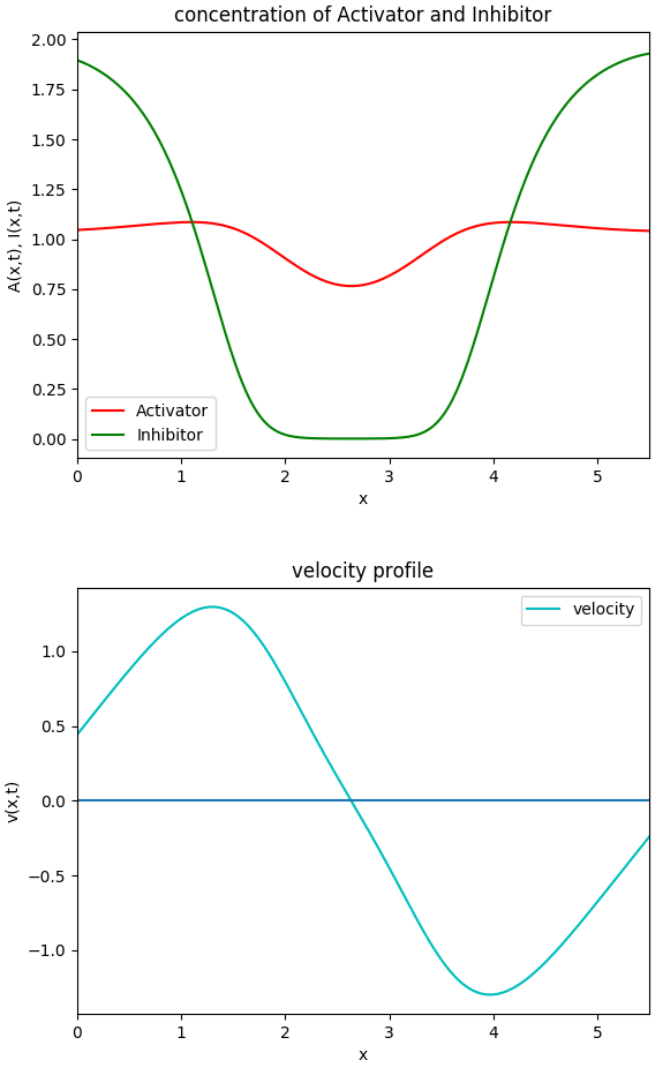

Figure 3.2: Oscillatory pattern. Concentration of I is represented by green and of A by blue. $\beta = 1.77$ and $\mathrm{Pe} = 1.4$.

3.3 Numerical solutions and Analysis

Let us take the coupled equations with the hydrodynamic flow and the two chemical species and solve them numerically in python with small perturbation about the homogeneous state for results. We have taken periodic boundary conditions with $L = 2\pi$ domain size and $\alpha = 0.1$. Saturation value of active stress are taken as $A_m = \zeta A_0$ and $I_m = \zeta I_0$.

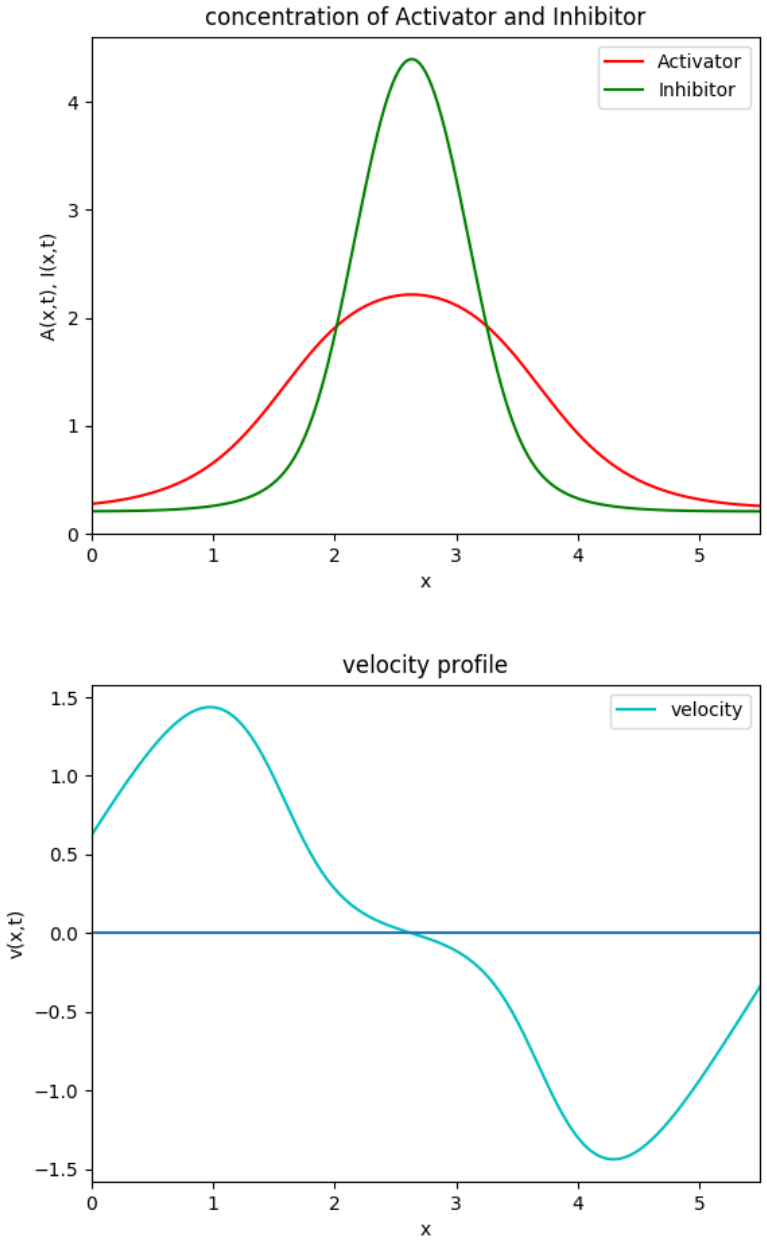

Figure 3.3: Sharpening of the peak due to convergent flow inside the region of I and A.

Fig. 3.1 shows that for different points in the phase space, we get different kind of patterns where the governing parameters are peclet number and β. There is an exciting thing to note that for massive Pe and $\beta > 1$, there is a transition from oscillatory patterns to stationary patterns. Now, for understanding the behavior of the concentrations of the activator and inhibitor, we choose some points from the

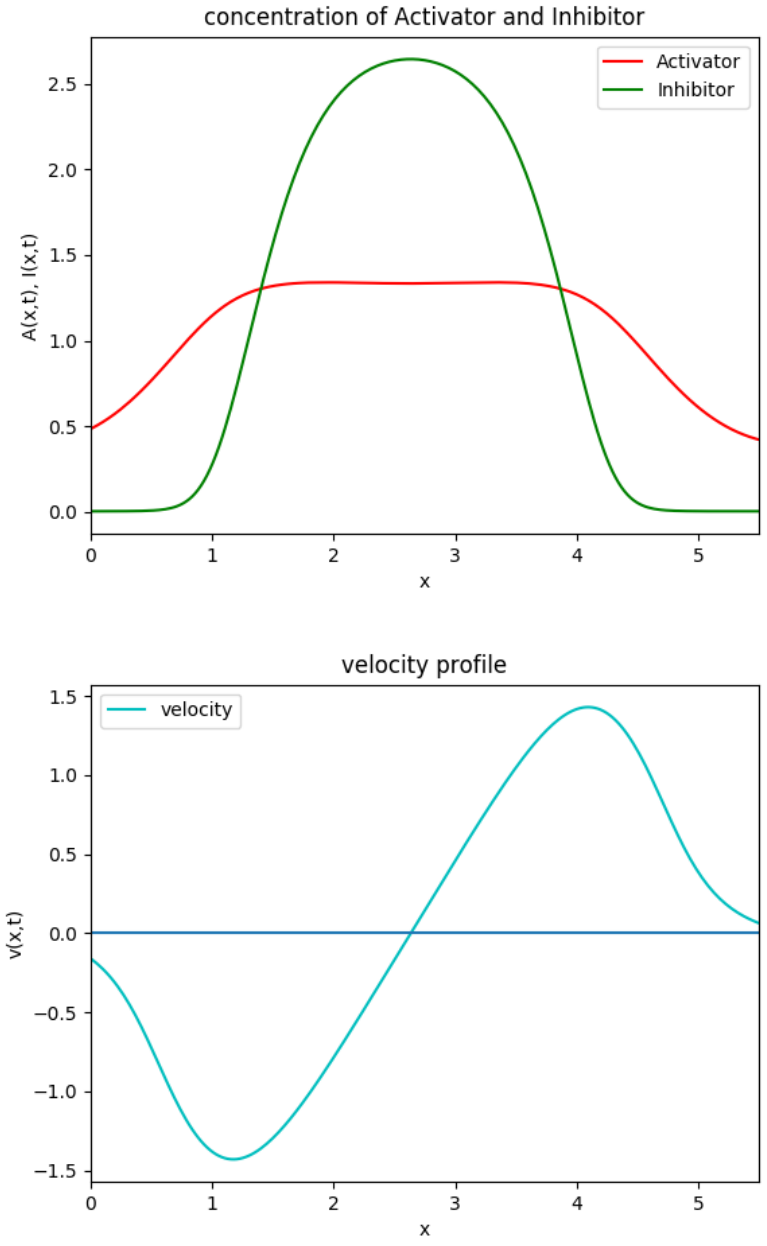

Figure 3.4: Flattening of the curve due to diffusion leading to divergent flows.

phase diagram and show the results obtained.

Fig. 3.2 shows that the concentration of inhibitor is low as compared to activator leading to convergent flows as active stress is higher. This hydrodynamic flow generated takes inhibitor and activator both to the region, where it forms a sharper peak due to less diffusivity Fig. 3.3. Further this reduces flow as active stress becomes less. These

peaks get shortened as hydrodynamic flow is less and gets relaxed by diffusion leading to divergent flows. The main point here is inhibitor peak remains high compared to activator as diffusion constant of I is less compared to A. Cycle is repeated again with specific time period.

Chapter 4

Role of Linear turnover for two chemical species

As discussed in Chapter 3, pulsatory patterns were regulated by the two chemical species with different diffusive relaxation time scales. In this, we will give a general overview of how we can introduce different relaxation time scales with linear turnover.

4.1 Including turnover

Consider two chemical species A and I discussed in the previous chapter now with linear chemical kinetics having the same diffusion constant but different linear turn over rates [9].

$$\partial_t A = -\partial_x(vA) + D_1\partial_x^2 A - k_1(A - A_0) \tag{4.1}$$

$$\partial_t I = -\partial_x(vI) + D_2\partial_x^2 I - k_2(I - I_0) \tag{4.2}$$

where k_1, k_2 gives the different relaxation rates of the activator and inhibitor. In our analysis, we choose $k_2/k_1 = \rho$. The forms of the active and passive stress remains the same as before. We again perform the linear stability analysis in the presence of turnover and the two chemical species to find the criterion of stable and unstable regimes.

4.2 Linear stability analysis for steady state

Let us consider the homogeneous steady state for the system under consideration where concentration is $c_0 = (A_0, I_0)$ and velocity is $v = 0$. To see whether the steady state is stable or unstable we perturb it from the steady state. Perturbations are taken of the form $c = c_0 + \delta c_0 e^{\iota \boldsymbol{k}\cdot\boldsymbol{x}}$. Proceeding as before, we obtain the following stability matrix in the presence of turnover

$$\tau\mathbb{L} = -k^2 l^2 \begin{pmatrix} 1 + \frac{1}{k^2 D} & 0 \\ 0 & 1 + \frac{\rho}{k^2 D} \end{pmatrix} + \frac{Pek^2 l^2}{1 + k^2 l^2} \begin{pmatrix} A_0 f_A & A_0 f_I \\ I_0 f_A & I_0 f_I \end{pmatrix}. \tag{4.3}$$

Note that the critical Pe_c will now be shifted in analogous way as we found in Chapter 2. Here we analyze the results obtained from the numerical simulations.

4.3 Numerical solution and Analysis

We considered two coupled advection-diffusion equations and incorporated linear turnover for both the equation in 1-D for periodic domain $L = 2\pi$.

$$\partial_t A = -\partial_x(vA) + D\partial_x^2 A - (A - A_0), \tag{4.4}$$

$$\partial_t I = -\partial_x(vI) + \alpha D\partial_x^2 I - \rho(I - I_0) \tag{4.5}$$

$$\eta\partial_x^2 v - \gamma v = -(\zeta\Delta\mu)_0 \partial_x f(c) \tag{4.6}$$

We choose $\alpha = 1$. Therefore, we have activator and inhibitor with same diffusion constants but linear turnover rates are different. The ratio of linear turnover rate of I and A is given by $\rho > 0$. Interestingly we observed pulsatory pattern if $\rho < 1$ which mean active stress up-regulator A turns over fast as compared to active stress down-regulator I. Different results were observed after solving above coupled equations numerically.

4.3.1 Stationary Pattern

In Fig. 4.1 we show that the patterns that are formed in the activator and inhibitor concentrations are stationary for low Pe.

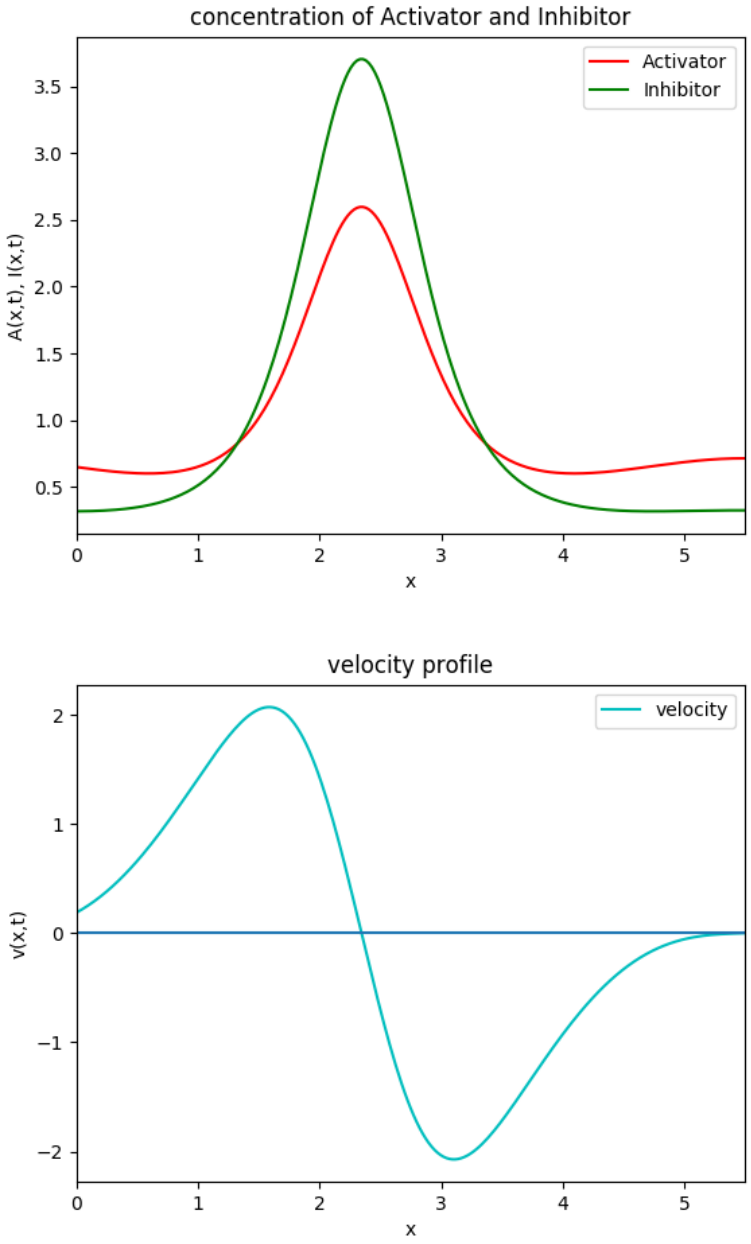

Figure 4.1: Stationary patterns for Activator and Inhibitor with linear turnover. $\beta = 1.4$, $Pe = 3.0$ and $\rho = 0.1$.

4.3.2 Drifting pattern with time

In Fig. 4.2 we show that the patterns that are formed in the activator and inhibitor concentrations are not stationary for higher Pe. The peaks move although the shapes are retained over time. Their velocity profiles also retain their shape as expected (not shown).

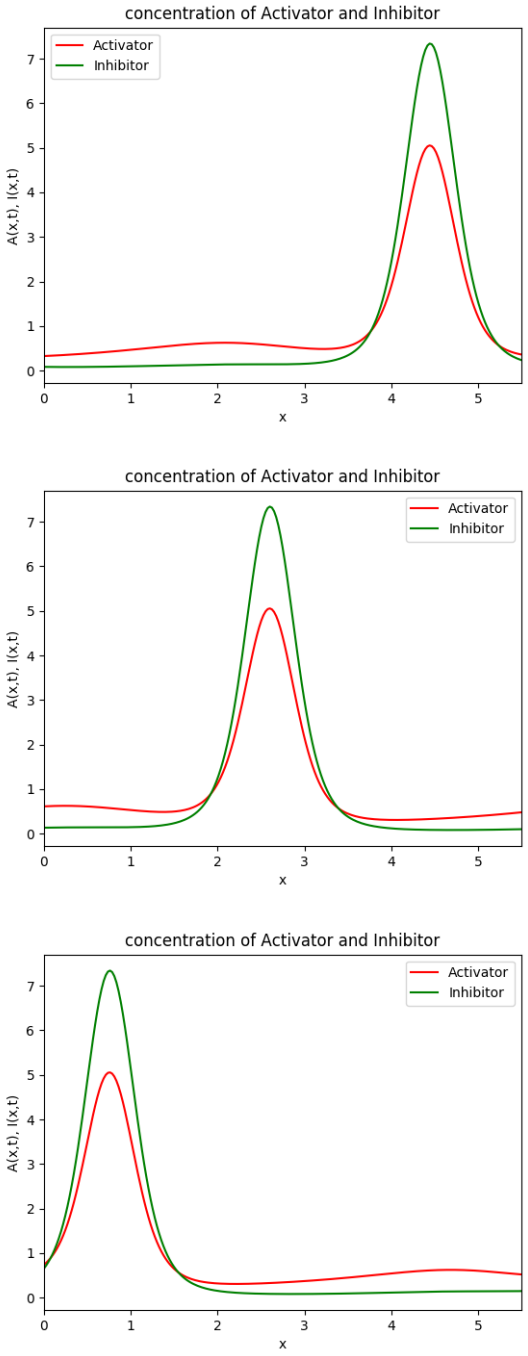

Figure 4.2:

4.3.3 Oscillatory pattern with time

Starting from the fig. 4.3 where we have the pattern formed in which inhibitor has a sharp peak as compared to the activator. This leads to a decrease in active stress for that particular region. Now, this reduces flows, and the concentration peaks began

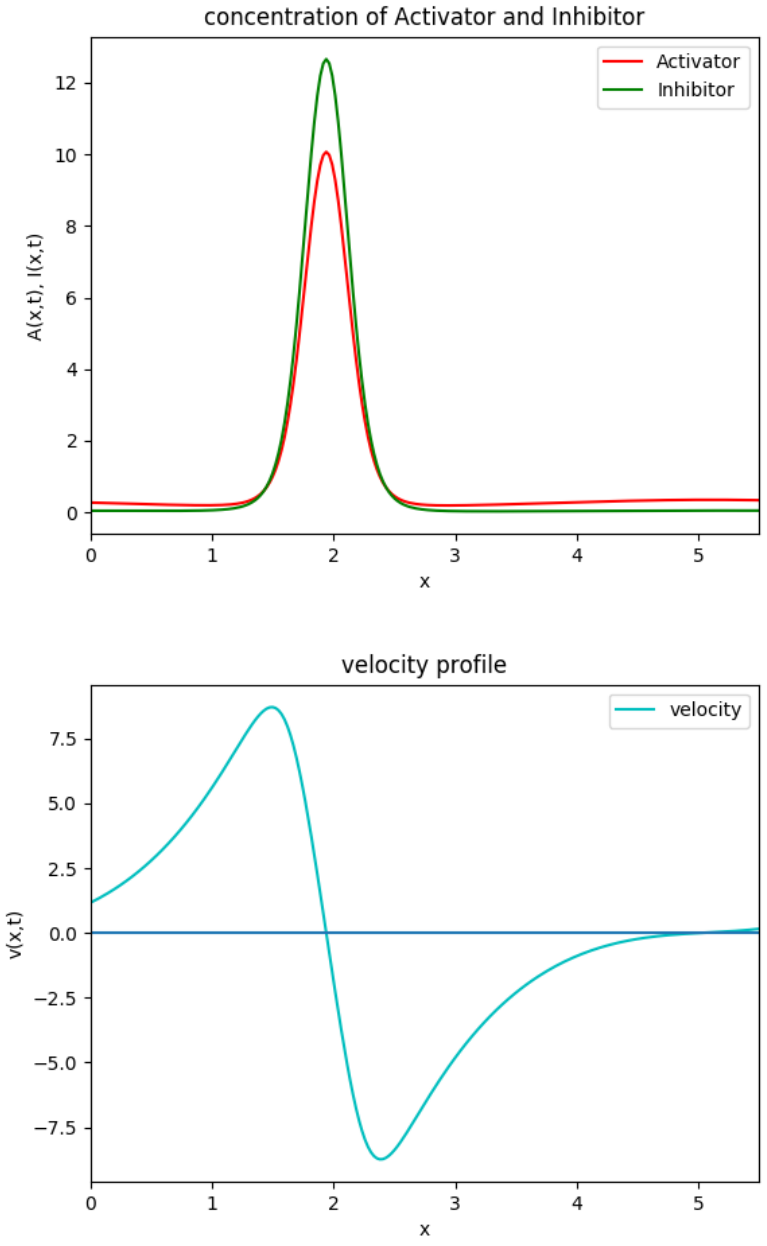

Figure 4.3: Concentration and velocity profile for activator and inhibitor at initial time t. Inhibitor is represented by green peak and activator by red.$\beta = 1.4$, pe $= 6.0$ and $\rho = 0.1$

to decline due to diffusion and linear turnover rate. We took diffusion constant to be same but linear turnover rates to be different by the ratio of $\rho = 0.1$ for inhibitor to activator. From fig. 4.4 we can see there is a decline in peak length for both activator and inhibitor, but there is more decline in the activator peak as it has a more linear turn over rate as compared to inhibitor. Now as the large peak goes down, there is a

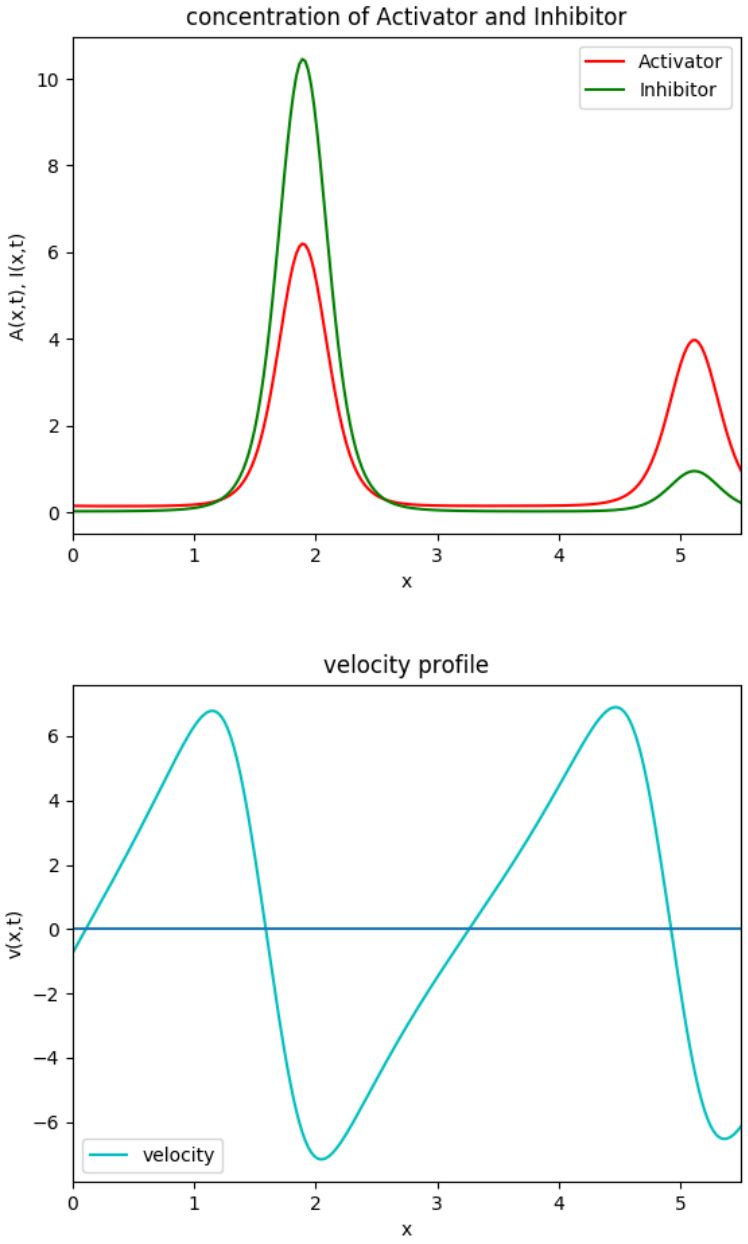

Figure 4.4: Decrease of peaks for both inhibitor and activator leading to the generation of small peak.

generation of another peak nearby, which is having activator to be more as compared to the inhibitor peak. Concentration for both species is conserved. In fig. 4.5 we see that the big pattern gets shifted towards left but also regains height with smaller peaks merging into it coming from left, and the lower peak to its right merge into another prominent peak onto its right. Further, this peak again goes down but also

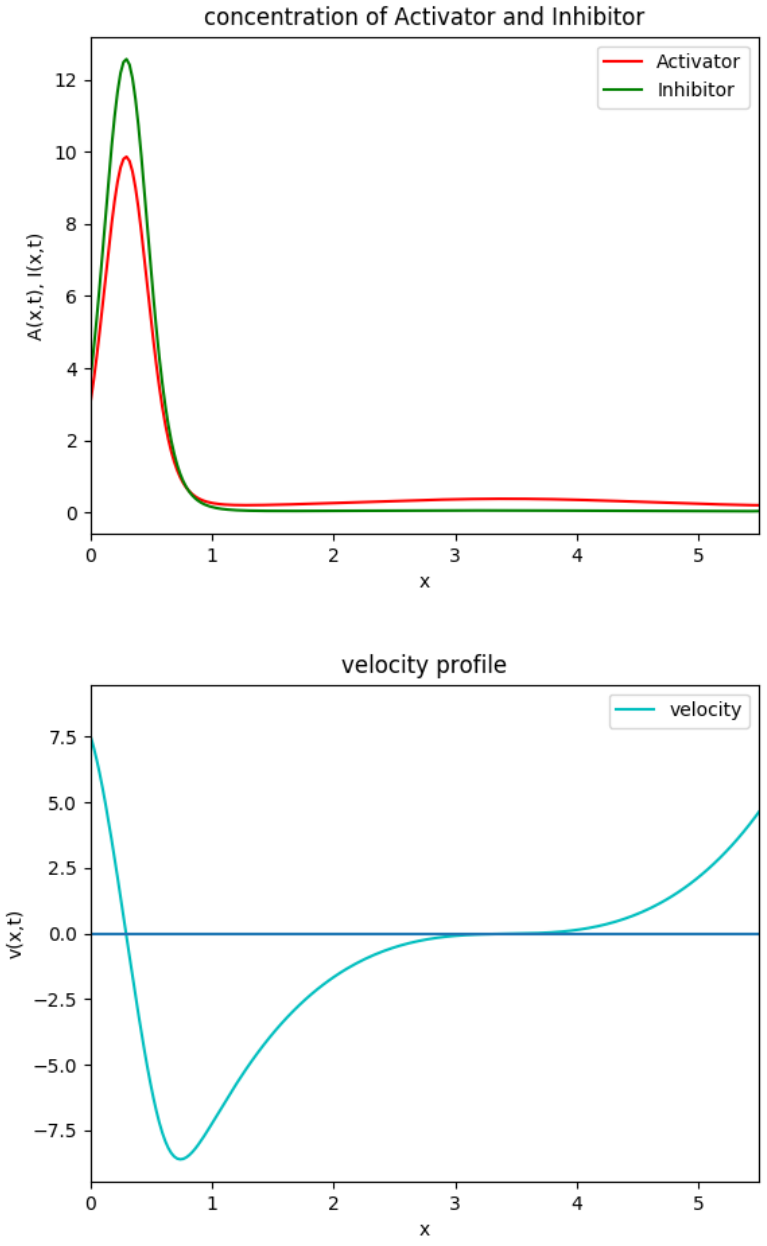

Figure 4.5: Oscillation of larger peak for both activator and inhibitor.

moves towards the right with the generation of the little peak which now after short time merges into the large peak and still comes back to fig. 4.3 which means this is a periodic cycle with a specific period.

We will explore the situation where we start with multiple peaks and see if they are stabilized in the presence of linear tunrnover of the activator and inhibitor. Further a

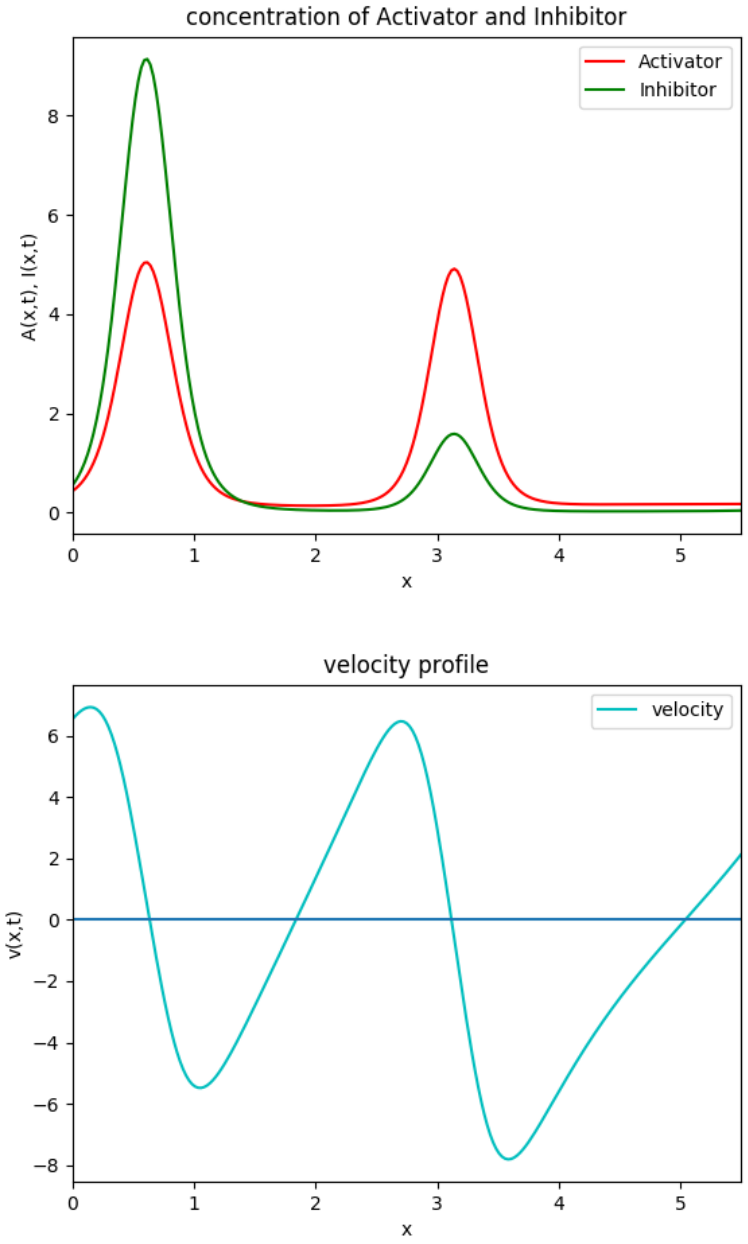

Figure 4.6: Merging of larger peak and smaller peak leading to the initial looking profile as seen in fig. 4.3

scan of the parameter space in ρ is also required to see the behavior. We are currently trying to build up the system for two dimensions.

Appendix A

Appendix Name

A.1 Spectral method for Equations

For approximating a derivative of the function numerically the simplest method what we use is Finite difference method. where for a given set of points y_i we have corresponding functional values as $f(y_i)$. The order of error is $O(h^2)$ and $0(h^4)$ which implies if we have more data points, the error will become less and approximation gets good. How is the spectral method different from finite difference method? So the answer to it is let say we have N number of points as N increases the error for finite difference, or finite element scheme decreases of the order $O(N^{-m})$ for some arbitrary constant m which is dependent upon the order of approximation and smoothness of the solution[10]. But on the other hand spectral method convergence is of the order $O(N^{-m})$ for every m is obtained given a condition function is infinitely differentiable and at faster convergence rate $O(c^N)(0 < c < 1)$[10].

Spectral methods use Fourier transformation technique. Fourier transform of a function f(x) is given by $\hat{f}(k)$

$$\hat{f}(k) = \int_{-\infty}^{+\infty} e^{-\iota kx} f(x)dx, \ (x \in \mathbb{R} \ \ and \ \ k \in \mathbb{R}) \tag{A.1}$$

Inverse Fourier transform is also used to reconstruct f(x) from $\hat{f}(k)$.

$$\hat{f}(x) = \frac{1}{2\pi} \int_{-\infty}^{+\infty} e^{\iota kx} \hat{f}(k) dk \tag{A.2}$$

If we have discretised points instead of the continuous function, then a Discrete Fourier transform method is used to evaluate the function. For a discretised periodic spatial domain we have points given as $x_j = jh$ with N as the number of points we will take N to be even(h $= x_{j+1} - x_j = \frac{2\pi}{N}$), on the other hand, wave number k will also be discretised, and the domain is bounded with the interval length $\frac{2\pi}{h}$ having the same number of point as in real space. Hence the interval is taken as $[\frac{-N}{2}, \frac{N}{2}]$.

$$\hat{f}(k) = h \sum_{j=1}^{N} e^{-\iota kx_j} fj, \quad k = -\frac{N}{2} + 1, ..., \frac{N}{2} \tag{A.3}$$

Also the inverse Fourier transform here is given as.

$$f(x) = \frac{1}{2\pi} \sum_{k=-\frac{N}{2}+1}^{\frac{N}{2}} e^{\iota kx_j} \hat{f}(k) \tag{A.4}$$

Discritised version is helpful when solving equations numerically for e.g. solving ODE, PDE etc. let us take v_j is the best approximation of $f_j^{'}$ which is the derivative of f with respect to the x. Now if we have a differential equation which is tough to solve, then we go in the Fourier space solve there and get the answer in real space by inverse Fourier transform. In Fourier space we can approximate the derivatives, for $f_j^{'}$ it will be $v_k = \iota k \hat{v}_k$ and if we want to approximate s_{th} derivative it would be $(\iota k)^s \hat{v}_k$. This technique helps to solve complicated time-dependent PDE in an easy manner with less error and computationally fast.

For e.g., if we have a PDE $\partial_x^2 u + \partial_x^4 u = 4$ to solve then doing with the finite difference method would be complicated but if we use the spectral method, it is easy. let us take this equation in Fourier space then the equation gets simplified to

$-k^2\hat{u}(k) + -k^4\hat{u}(k) = 4$ now we have value of function at each wavenumber. For getting the exact solution, we take the inverse Fourier transform of the function.

A.2 Spectral method for one chemical species

The coupled equations used for numerical simulations are.

$$\partial_t c = -\partial_x(vc) + D\partial_x^2 c \tag{A.5}$$

$$\eta\partial_x^2 v - \gamma v = -(\zeta\Delta\mu)_0\partial_x f(c) \tag{A.6}$$

Here $f(c) = \frac{c}{c+1}$. Solving these equations give the required pattern.

A.2.1 Code for simulation

```
#Pattern formation in active fluids in 1-D with active flows v(x,t) and diffusion
one-species concentration c(x,t) like myosin flows in actomyosin cortex in cell
import numpy as np
import scipy.fftpack as fft
import time
from scipy.integrate import odeint
import matplotlib.pyplot as plt
from scipy.interpolate import interp1d
from matplotlib.widgets import Slider
length = 2.0*np.pi
s_len = 1.0
nx = 256
x = np.arange(0.0,length,length/nx)
times = np.linspace(0,100.0,100.0)
c0 = 1.0
D = 1.0
gamma = 1.0
zeta_del_mu_not = 16
k = fft.rfftfreq(nx, length / (2.0*np.pi*nx))
k_sq = k**2
pole = 1.0/(gamma * s_len**2 * (s_len**(-2) + k_sq))
```

```
def Active_Stress(c,t):
    active_stress = zeta_del_mu_not * (c / (1.0 + c))
    return active_stress

def flow_velocity(c,t):
    active_stress1 = Active_Stress(c, t)
    dx_active_stress = fft.diff(active_stress1, order=1, period=length)
    v_x = fft.irfft(fft.rfft(dx_active_stress) * pole)
    return np.real(v_x)

def time_derivative(c,t):
    vx = flow_velocity(c,t)
    dcdt = np.real(-fft.diff(vx * c, order=1, period=length) +
                        D * fft.diff(c, order=2, period=length))
    return dcdt

c_int = c0 * (np.ones_like(x) + 0.01*(1-2*np.random.rand(nx)))
c = odeint(time_derivative, c_int, times)
vx = np.zeros_like(c)
for i in range(len(times)):
    vx[i,:] = flow_velocity(c[i,:], times[i])

fig, ax = plt.subplots(1, sharex=True, figsize=(8,6))
fig.subplots_adjust(left=0.15, bottom=0.1, top=0.92, right=0.94,
                wspace=0.3, hspace=0.1)
ax.set_xlabel('c(x,t), vx(x,t)')
ax.set_ylabel('x')
ax.set_ylim(min(c.min(), vx.min()), max(c.max(),vx.max()))
ax.set_xlim(0, length)
ax.get_xaxis().set_label_coords(0.5,-0.15)
ax.get_yaxis().set_label_coords(0.5,-0.15)
ax.grid(False)
cline, = ax.plot(x, c[0,:], color='#659CEF',lw=1.5,)
vxline, = ax.plot(x, vx[0,:], color='#7DBD00', lw=1.5)
```

```
def update(val):
    ti = (abs(times-val)).argmin()
    cline.set_ydata(c[ti,:])
    vxline.set_ydata(vx[ti,:])
    plt.draw()

sax=plt.axes([0.125, 0.95, 0.75, 0.015])
slider = Slider(sax, 't', min(times), max(times), valinit=min(times), valfmt='%+4.1
,fc='#999999')
slider.drawon = False
slider.on_changed(update)
plt.legend(loc='best')
plt.show()

plt.plot(x,c[99,:],'b-',label='Concentration')
plt.plot(x,vx[99,:],'g-',label='Velocity')

plt.ylabel('C(x,t),v(x,t)')
plt.xlabel('x')
plt.legend(loc='best')
plt.show()
```

A.3 Spectral method for two chemical species

Here we have three coupled equations two equations are of concentration field and one is hydrodynamical flow. Solving them numerically gives the required patterns.

$$\partial_t A = -\partial_x(vA) + D\partial_x^2 A, \tag{A.7}$$

$$\partial_t I = -\partial_x(vI) + \alpha D\partial_x^2 I, \tag{A.8}$$

$$\eta\partial_x^2 v - \gamma v = -(\zeta\Delta\mu)_0\partial_x f(c) \tag{A.9}$$

Here $f(c) = (1+\beta)\frac{A}{A+A_m} + (1-\beta)\frac{I}{I+I_m}$.

A.3.1 Code for simulation

```
#Pattern formation in active fluids in 1-D with active flows v(x,t) and
diffusion for 2-species concentrations A(x,t) and I(x,t) like myosin flows in actomyos
cortex in cell
import numpy as np
import scipy.fftpack as fft
import time
from scipy.integrate import odeint
import matplotlib.pyplot as plt
from scipy.interpolate import interp1d
from matplotlib.widgets import Slider
length = 2.0*np.pi
s_len = 1.0
nx = 256
beta = 2.5
x = np.arange(0.0,length,length/nx)
times = np.linspace(0,200.0,200.0)
D = 1.0
D1 = 0.1
A_S = 3.0
I_S = 3.0
gamma = 1.0
zeta_del_mu_not = 0.6
k = fft.rfftfreq(nx, length / (2.0*np.pi*nx))
k_sq = k**2
pole = 1.0/(gamma * s_len**2 * (s_len**(-2) + k_sq))

def Active_Stress(c,t):
    A, I = np.split(c, 2)
    active_stress = zeta_del_mu_not * (16.0/3.0) * ((1 + beta) * (A / (A_S + A)) +
    (1 - beta) * (I/ (I_S + I)))
```

```
    return active_stress

def flow_velocity(c,t):
    active_stress1 = Active_Stress(c, t)
    dx_active_stress = fft.diff(active_stress1, order=1, period=length)
    v_x = fft.irfft(fft.rfft(dx_active_stress) * pole)
    return np.real(v_x)

def time_derivative(c,t):
    A, I = np.split(c, 2)
    vx = flow_velocity(c,t)
    dAdt = np.real(-fft.diff(vx * A, order=1, period=length) +
                        D * fft.diff(A, order=2, period=length))
    dIdt = np.real(-fft.diff(vx * I, order=1, period=length) +
                        D1 * fft.diff(I, order=2, period=length))
    return np.concatenate([dAdt, dIdt])

ssvals = (1.0, 1.0)
c_int = np.concatenate(np.array([ss * np.ones(nx) + 0.01*(1-2*np.random.rand(nx)) f
ssvals]))
c = odeint(time_derivative, c_int, times)
A_x, I_x = np.split(c, 2, axis=1)
vx = np.zeros_like(A_x)
for i in range(len(times)):
    vx[i,:] = flow_velocity(c[i,:], times[i])

fig, ax = plt.subplots(1, sharex=True, figsize=(8,6))
fig.subplots_adjust(left=0.15, bottom=0.1, top=0.9, right=0.94,
                wspace=0.3, hspace=0.1)
ax.set_xlabel('x')
ax.set_ylabel('c(x,t), vx(x,t)')
ax.set_title('Velocity Profile')
ax.set_ylim(min(vx.min(), I_x.min()), max(vx.max(),I_x.max()))
ax.set_xlim(0, length)
ax.get_xaxis().set_label_coords(0.5,-0.15)
```

```
ax.get_yaxis().set_label_coords(0.5,-0.15)
ax.grid(False)
cline, = ax.plot(x, vx[0,:], color='#659CEF',lw=1.5,)
vxline, = ax.plot(x, I_x[0,:], color='#7DBD00', lw=1.5)
def update(val):
    ti = (abs(times-val)).argmin()
    cline.set_ydata(vx[ti,:])
    vxline.set_ydata(0)
    plt.draw()

sax=plt.axes([0.125, 0.95, 0.75, 0.015])
slider = Slider(sax, 't', min(times), max(times), valinit=min(times), valfmt='%+4.2f'
,fc='#999999')
slider.drawon = False
slider.on_changed(update)
plt.legend(loc='best')
plt.show()

fig, ax = plt.subplots(1, sharex=True, figsize=(8,6))
fig.subplots_adjust(left=0.15, bottom=0.1, top=0.9, right=0.94,
                wspace=0.3, hspace=0.1)
ax.set_xlabel('c(x,t), vx(x,t)')
ax.set_ylabel('x')
ax.set_title('concentration of Activator and Inhibitor')
ax.set_ylim(min(A_x.min(), I_x.min()), max(A_x.max(),I_x.max()))
ax.set_xlim(0, length)
ax.get_xaxis().set_label_coords(0.5,-0.15)
ax.get_yaxis().set_label_coords(0.5,-0.15)
ax.grid(False)
cline, = ax.plot(x, A_x[0,:], color='#659CEF',lw=1.5,)
vxline, = ax.plot(x, I_x[0,:], color='#7DBD00', lw=1.5)
def update(val):
    ti = (abs(times-val)).argmin()
    cline.set_ydata(A_x[ti,:])
    vxline.set_ydata(I_x[ti,:])
```

```
    plt.draw()

sax=plt.axes([0.125, 0.95, 0.75, 0.015])
slider = Slider(sax, 't', min(times), max(times), valinit=min(times), valfmt='%+4.2
,fc='#999999')
slider.drawon = False
slider.on_changed(update)
plt.legend(loc='best')
plt.show()
```

Bibliography

[1] Peter Gross, K Vijay Kumar, and Stephan W Grill. How active mechanics and regulatory biochemistry combine to form patterns in development. *Annual review of biophysics*, 46:337–356, 2017.

[2] Len M Pismen. *Patterns and interfaces in dissipative dynamics*. Springer Science & Business Media, 2006.

[3] A Turing. The chemical basis of morphogenesis, phil. trans. roy. soc. b, 237 (1952), 37-72. *Reprinted in Bull. Math. Biol*, 52:153–197, 1990.

[4] Howard C Berg. *Random walks in biology*. Princeton University Press, 1993.

[5] Michael Cross and Henry Greenside. *Pattern formation and dynamics in nonequilibrium systems*. Cambridge University Press, 2009.

[6] Pierre Recho, Adrien Hallou, and Edouard Hannezo. Theory of mechanochemical patterning in biphasic biological tissues. *Proceedings of the National Academy of Sciences*, 116(12):5344–5349, 2019.

[7] Justin S Bois, Frank Jülicher, and Stephan W Grill. Pattern formation in active fluids. *Physical review letters*, 106(2):028103, 2011.

[8] Mirjam Mayer, Martin Depken, Justin S Bois, Frank Jülicher, and Stephan W Grill. Anisotropies in cortical tension reveal the physical basis of polarizing cortical flows. *Nature*, 467(7315):617–621, 2010.

[9] K Vijay Kumar, Justin S Bois, Frank Jülicher, and Stephan W Grill. Pulsatory patterns in active fluids. *Physical Review Letters*, 112(20):208101, 2014.

[10] Lloyd N Trefethen. *Spectral methods in MATLAB*, volume 10. Siam, 2000.

[11] Frank Jülicher, Stephan W Grill, and Guillaume Salbreux. Hydrodynamic theory of active matter. *Reports on Progress in Physics*, 81(7):076601, 2018.